

Supporting Information

Transition from Isotropic Positive to Negative Thermal Expansion by Local Zr_6O_8 Node Distortion in MOF-801

Rui Ma,^a Zhanning Liu,^{b,*} Liang Chen,^a Qiang Li,^a Kun Lin,^a Xin Chen,^a Jinxia Deng,^a Koji Ohara,^c and Xianran Xing^{a,*}

^a Beijing Advanced Innovation Center for Materials Genome Engineering, Institute of Solid State Chemistry, University of Science and Technology Beijing, Beijing 100083, China

^b School of Materials Science and Engineering, Shandong University of Science and Technology, Qingdao, 266590, China

^c Diffraction and Scattering Division, Center for Synchrotron Radiation Research, Japan Synchrotron Radiation Research Institute, Sayo-cho, Sayo-gun, Hyogo 679-5198, Japan

Supplementary Figures and Tables

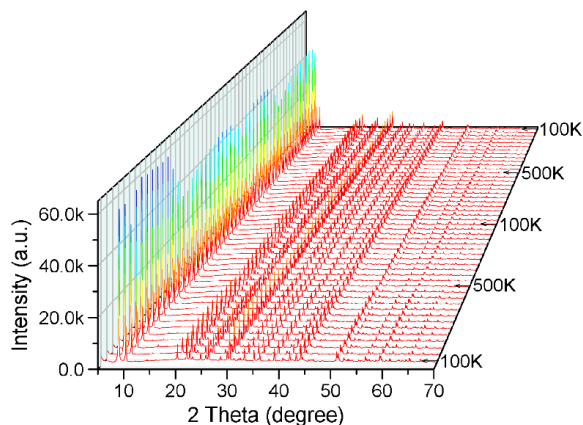


Figure S1. Cyclic temperature-dependent X-ray diffraction patterns were collected from 100 K to 500 K in MOF-801, containing cycles of both heating and cooling.

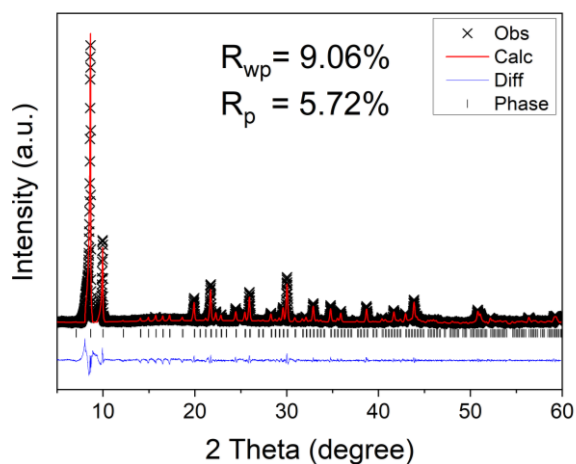


Figure S2. Rietveld refinement pattern of MOF-801 at 300K.

Table S1. The coefficients of some representative NTE MOFs.

Compound	CTE	Temperature range (K)	Reference
MOF-5	$\alpha_a = -13.1 \text{ MK}^{-1}$	100~500	1
$\text{Cu}_3(\text{BTC})_2$	$\alpha_a = -4.1 \text{ MK}^{-1}$	80~500	2
$\text{TCNQ}@ \text{Cu}_3(\text{BTC})_2$	$\alpha_a = -2.8 \text{ MK}^{-1}$	100~300	3
MOF-14	$\alpha_a = -4 \sim -13.1 \text{ MK}^{-1}$	3~400	4
MIL-68(In)	$\alpha_a = -5.6 \text{ MK}^{-1}$ $\alpha_b = -2.7 \text{ MK}^{-1}$ $\alpha_c = -4.0 \text{ MK}^{-1}$	125~600	5
Ca-sq	$\alpha_a = -4.7 \text{ MK}^{-1}$ $\alpha_b = -0.1 \text{ MK}^{-1}$	100~450	6
Cd-sq	$\alpha_a = -14.3 \text{ MK}^{-1}$ $\alpha_c = +14.8 \text{ MK}^{-1}$	100~350	7
Cd(trz)	$\alpha_a = -12.2 \sim -3.5 \text{ MK}^{-1}$ $\alpha_c = +10.4 \sim +18.2 \text{ MK}^{-1}$	100~550	8
MOF-808- SO_4	$\alpha_a = -39.7 \text{ MK}^{-1}$	25~250	9
UiO-66(Hf)	$\alpha_a = -32.3 \text{ MK}^{-1}$	433~613	10
$[\text{Zr}_6\text{O}_4(\text{OH})_4(\text{c} \text{ dba})_6]$	$\alpha_a = -11.0 \text{ MK}^{-1}$	127~434	11
NU-1000-formate	$\alpha_a = -30.0 \text{ MK}^{-1}$	at 443	12
MOF-801	$\alpha_a = -31.6 \text{ MK}^{-1}$	375~500	This work

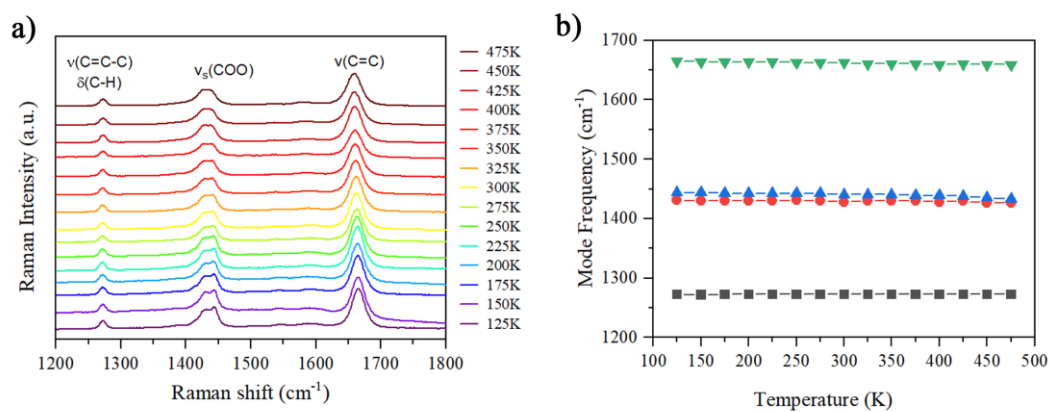


Figure S3. a) The zoomed part of *in situ* variable temperature Raman spectra of MOF-801 and b) the corresponding peak center.

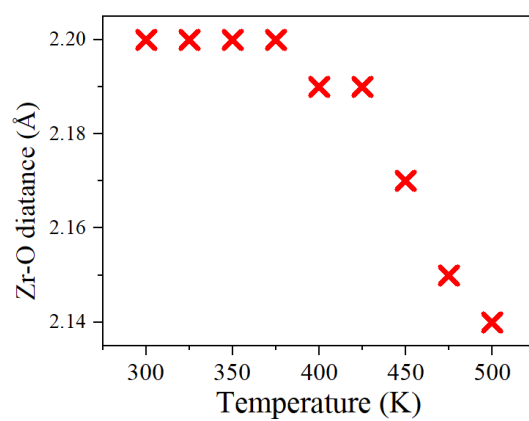


Figure S4. The change of Zr-O distance extracted from variable temperature PDF patterns.

References:

1. Lock, N.; Wu, Y.; Christensen, M.; Cameron, L. J.; Peterson, V. K.; Bridgeman, A. J.; Kepert, C. J.; Iversen, B. B., Elucidating negative thermal expansion in MOF-5. *The Journal of Physical Chemistry C* **2010**, *114* (39), 16181-16186.
2. Wu, Y.; Kobayashi, A.; Halder, G. J.; Peterson, V. K.; Chapman, K. W.; Lock, N.; Southon, P. D.; Kepert, C. J., Negative Thermal Expansion in the Metal–Organic Framework Material Cu₃(1, 3, 5-benzenetricarboxylate) 2. *Angewandte Chemie International Edition* **2008**, *47* (46), 8929-8932.
3. Schneider, C.; Bodesheim, D.; Ehrenreich, M. G.; Crocellà, V.; Mink, J.; Fischer, R. A.; Butler, K. T.; Kieslich, G., Tuning the negative thermal expansion behavior of the metal–organic framework Cu₃BTC₂ by retrofitting. *Journal of the American Chemical Society* **2019**, *141* (26), 10504-10509.
4. Wu, Y.; Peterson, V. K.; Luks, E.; Darwish, T. A.; Kepert, C. J., Interpenetration as a Mechanism for Negative Thermal Expansion in the Metal–Organic Framework Cu₃(btb)₂ (MOF-14). *Angewandte Chemie* **2014**, *126* (20), 5275-5278.
5. Liu, Z.; Li, Q.; Zhu, H.; Lin, K.; Deng, J.; Chen, J.; Xing, X., 3D negative thermal expansion in orthorhombic MIL-68 (In). *Chemical Communications* **2018**, *54* (45), 5712-5715.
6. Liu, Z.; Wang, Z.; Sun, D.; Xing, X., Intrinsic volumetric negative thermal expansion in the “rigid” calcium squarate. *Chemical Communications* **2021**, *57* (74), 9382-9385.
7. Liu, Z.; Ma, R.; Deng, J.; Chen, J.; Xing, X., Molecular packing-dependent thermal expansion behaviors in metal squarate frameworks. *Chemistry of Materials* **2020**, *32* (7), 2893-2898.
8. Liu, Z.; Fan, L.; Xing, C.; Wang, Z., Negative Thermal Expansion in the Noncarboxylate Based Metal–Organic Framework Cd (trz) Cl. *ACS Materials Letters* **2023**, *5*, 1911-1915.
9. Baxter, S. J.; Mendez-Arroyo, J.; Enterkin, J.; Alvey, P. M.; May, C.; Cox, C.; Yao, J., The effects of ligand substitution on MOF-808 thermal cycling stability and negative thermal expansion. *ACS Materials Letters* **2022**, *4* (11), 2381-2387.
10. Cliffe, M. J.; Hill, J. A.; Murray, C. A.; Coudert, F.-X.; Goodwin, A. L., Defect-dependent colossal negative thermal expansion in UiO-66 (Hf) metal–organic framework. *Physical Chemistry Chemical Physics* **2015**, *17* (17), 11586-11592.
11. Zhou, H. L.; Bai, J.; Ye, J. W.; Mo, Z. W.; Zhang, W. X.; Zhang, J. P.; Chen, X. M., Thermal and Gas Dual-Responsive Behaviors of an Expanded UiO-66-Type Porous Coordination Polymer. *ChemPlusChem* **2016**, *81* (8), 817-821.
12. Chen, Z.; Stroschio, G. D.; Liu, J.; Lu, Z.; Hupp, J. T.; Gagliardi, L.; Chapman, K. W., Node Distortion as a Tunable Mechanism for Negative Thermal Expansion in Metal–Organic Frameworks. *Journal of the American Chemical Society* **2022**, *145* (1), 268-276.